Journal of Earth Science, *Vol. 28*, *No. 4*, *p. 729–738*, *August 2017* *ISSN 1674-487X*
Printed in China
DOI: 10.1007/s12583-017-0756-2

Analysis of Atmospheric Turbidity in Clear Skies at Wuhan, Central China

Lunche Wang*[1], Yisen Chen[1], Ying Niu[1], Germán Ariel Salazar[2], Wei Gong[3]
1. *Department of Geography*, *School of Earth Sciences*, *China University of Geosciences*, *Wuhan* 430074, *China*
2. *Physics Department*, *School of Exact Sciences*, *Salta National University*, *Salta A*4408*FVY*, *Argentina*
3. *State Key Laboratory of Information Engineering in Surveying*, *Mapping and Remote Sensing*, *Wuhan University*, *Wuhan* 430079, *China*
Lunche Wang: http://orcid.org/0000-0001-7783-5725

ABSTRACT: The Ångström turbidity coefficient (β) and Linke turbidity factor (T_L) are used to study the atmospheric conditions in Wuhan, Central China, using measured direct solar radiation during 2010–2011 in this study. The results show that annual mean β values generally increase from 0.28 in the morning to 0.35 at noon, and then decrease to 0.1 in the late afternoon during the day; annual mean T_L generally varies from 3 to 7 in Central China. Both turbidity coefficients have maximum values in spring and summer, while minimum values are observed in winter months. It also reveals that β values show preponderance (52.8%) between 0.15 and 0.35, 78.1% of T_L values are between 3.3 and 7.7, which can be compared with other sites around the world. Relationship between turbidity coefficients and main meteorological parameters (humidity, temperature and wind direction) have been further investigated, it is discovered that the local aerosol concentrations, dust events in northern China and Southwest Monsoon from the Indian Ocean influences the β values in the study area.
KEY WORDS: direct solar radiation, Ångström turbidity coefficient, Linke turbidity factor, Central China.

0 INTRODUCTION

Solar radiation on Earth's surface is the primary energy source for life on our planet (Wang et al., 2016; Wild et al., 2005; Leckner, 1978), which is attenuated through the atmosphere due to the presence of air molecules, clouds, and aerosols (Lin et al., 2016; Trenberth et al., 2009; Braslau and Dave, 1973). There are two major attenuation mechanisms taking place, namely, the absorption and scattering process (Malik, 2000; Iqbal, 1983). This attenuation process can be described using an index of atmospheric turbidity, which is directly related to the effects of cloud, aerosol and other atmospheric compositions on the surface solar radiation (Wang et al., 2015a; Gueymard, 2005; Li and Lam, 2002; Ångström, 1961). Due to the great spatial-temporal variations of cloud and aerosols, the associated radiative forcing effects in regional or global scale also differ greatly from site to site (Mavromatakis and Franghiadakis, 2007; Power, 2001). Therefore, it is necessary to study the distributions and sources of atmospheric turbidity in different places, which is of vital importance for climate modeling and energy applications (Li et al., 2016; Pan et al., 2016; Ellouz et al., 2013; Adamopoulos et al., 2007; López and Batlles, 2004).

The parameters that characterize the atmospheric turbidity are called turbidity coefficients (Wang et al., 2015b; El-Metwally, 2013; Dogniaux, 1974; Ångström, 1964). In recent decades, Linke turbidity factor T_L and Ångström turbidity coefficient β are the most commonly used turbidity coefficients (Salazar et al., 2013). T_L describes the optical thickness of the atmosphere due to both absorption by water vapor and absorption and scattering by aerosol particles in a dry and clean atmosphere (Linke, 1922); β represents the amount of aerosol present in the air in the vertical direction (Gueymard and Garrison, 1998; Grenier et al., 1995; Ångström, 1961). Both indices have been widely used in meteorological observations and related atmospheric environment studies in the world (Salazar, 2011; Wen and Yeh, 2009; Kaskaoutis and Kambezidis, 2007; Sapkota and Dhaubhadel, 2002).

Many studies have been conducted to investigate the variations of T_L and β around the world, there are generally two ways: observation of spectral radiation data using sun photometers or spectroradiometers (Bilbao et al., 2014; Ellouz et al., 2013; Janjai et al., 2003), and measurements of broadband solar radiation using radiometer (Djafer and Irbah, 2013; Wen and Yeh, 2009). For example, Xia et al. (2007) analyzed the aerosol optical properties and the related radiative effects in Yangtze Delta region of China using CE318 sun photometer; Che et al. (2015) discussed the aerosol climatology of China during 2002–2013 in detail using observations from China Aerosol Remote Sensing Network. But these instruments are expensive and difficult to maintain, which limits its applications and long-term studies (Wang et al., 2015b; El-Metwally, 2013; Chaâbane, 2008; Hussain et al., 2000). The turbidity

*Corresponding author: wang@cug.edu.cn

Manuscript received January 25, 2017.
Manuscript accepted March 20, 2017.

coefficients estimating from broadband solar radiation are easy to conduct in recent years due to the routine radiation observations (and enough calibration and maintenance techniques) in automatic weather station (Lin et al., 2016; Trabelsi and Masmoudi, 2011; Li and Lam, 2002), for example, Louche et al. (1987) determined the value of β with direct normal irradiance (DNI) from Ajaccio (France); Hussain et al. (2000) analyzed the atmospheric turbidity in Bangladesh; Trabelsi and Masmoudi (2011) analyzed the atmospheric turbidity over Kerkennah Island in Tunisia; Djafer and Irbah (2013) investigated the turbidity over Ghardaïa City using five-year solar irradiance and meteorological observations; Bilbao et al. (2014) calculated the value of β from normal direct solar irradiance in Central Spain. Due to the worldwide network for observing solar radiation since 1990s, it provides a practical method for atmospheric turbidity study at different locations around the world.

Many researchers have investigated the turbidity coefficients from solar radiation, however, most of the studies are mainly focused on North America, South America, Europe, Indian and Africa, and very little work has been carried out in China, especially in large areas of Central China (Wang et al., 2015c). The turbidity issues in China have attracted great attentions from scientific community and the public due to the frequent occurrences of haze and air pollution event in recent years (Wang Y Q et al., 2015), which further promote this study to analyze the turbidity conditions in different sites.

Wuhan, a total population near 12 million, was chosen to determine and analyze both turbidity coefficients from 10-minute solar radiation observations during 2010–2011. It is the first time to investigate the atmospheric turbidity under clear sky conditions at Wuhan using ground based broadband solar radiation data. Diurnal, monthly and seasonal variations of turbidity coefficients will be presented and discussed in detail. The correlations between meteorological parameters and the turbidity coefficients will also be analyzed in this paper.

1 MATERIALS AND METHODS

1.1 Site Descriptions and Instruments

The observation site is located in Wuhan University (WHU) (latitude 30°32′N, longitude 114°21′E and 30 m a.s.l.), Wuhan, Hubei province, China, the detailed Geographical location can be seen in Fig. 1. The rapid growth of urbanization has led to heavy emissions of anthropogenic pollutants in recent decades, and the main aerosol sources in this study area are pollutant emissions from industrial manufacturing, traffic systems, and cooking using fossil fuels (Gong et al., 2015; Wang et al., 2014a; Feng et al., 2010). The measurement system consists of instruments for measuring global solar radiation (measured by CM-21 pyranometer), direct radiation (CH-1 direct radiometer) and diffuse radiation (CM-11 global radiometer associated with a 2-AP sun tracker) and some other meteorological parameters. All radiation values were recorded at 1-minute time intervals, hourly and daily values were then derived from the minute values via integration (Wang et al., 2013; Hu et al., 2007). The calibrations for the radiometers have been conducted each year at the calibration centre in Beijing, China, the detailed process has been described in previous studies Hu et al. (2007) and Wang et al. (2016, 2014b).

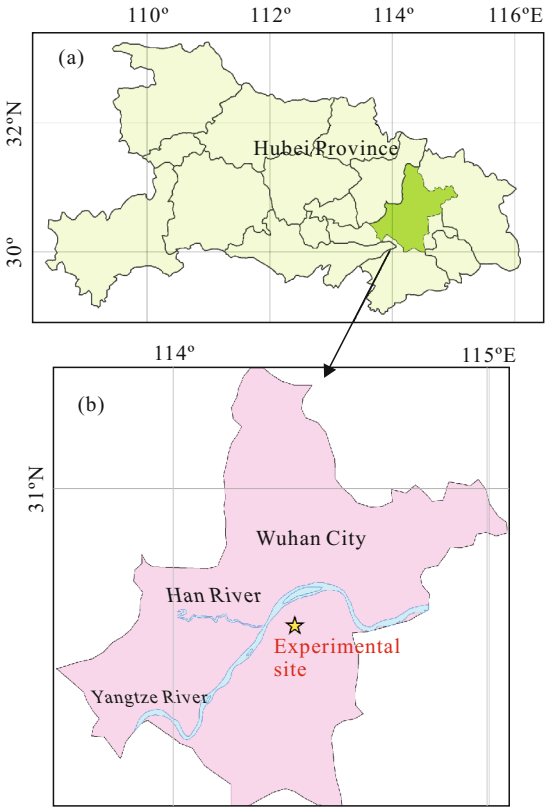

Figure 1. Sketch maps showing the geographical location of the study site WHU. (a) Location of Wuhan in Hubei Province; and (b) WHU site in Wuhan.

The global, direct and diffuse solar irradiance for zenith solar angles (θ_z) lower than 80° was considered and analyzed from January 2010 to December 2011 in this study. The method of Long and Ackerman (2000) has been used for selecting data under clear skies; data with direct normal irradiance less than 200 $W \cdot m^{-2}$ was also ignored in the selection. Finally, 35% of the whole data set remains in the present study. Table 1 shows the monthly mean meteorological parameters during 2010–2011 at Wuhan. It is clear that air temperature generally increased from winter to summer months; most of the rainfall concentrates in summer (from June to August) months, for example, rainfall amount (433.9 mm) in June takes about 44% of the whole rainfall in 2011. Monthly sunshine hours also increased from winter to summer months; the wind speed ranges from 1.31 to 3.01 $m \cdot s^{-1}$ throughout the year.

1.2 Ångström Turbidity Coefficient β

Ångström (1961) proposed the transmission of incident solar radiation due to the effects of aerosols expressing as

$$\tau_{a,\lambda}=\exp(-\beta\lambda^{-\alpha}m) \quad (1)$$

where β is the turbidity coefficient related to the concentration of aerosols in the air, α is the Ångström exponent related to the size distribution of the aerosols (large values of α indicate a relatively high ratio of small particles to large particles), λ is the wavelength of the incident radiation and m is the relative optical air mass (Wang et al., 2015c; Djafer and Irbah, 2013). The values of β vary throughout the day due to photochemical activity,

Table 1 Monthly mean values of atmospheric parameters at Wuhan, China during 2010–2011

Month	Temperature (ºC)		Humidity (%)		Rainfall (mm)		Wind speed ($m \cdot s^{-1}$)		Sunshine (h)	
	2010	2011	2010	2011	2010	2011	2010	2011	2010	2011
January	4.23	0.73	79.77	62.58	28.5	15.6	2.07	1.94	70.1	106.5
February	6.64	6.04	83.75	70.11	49.5	19.2	2.26	1.99	65	109.3
March	10.36	10.28	74.52	63.68	150.6	32.1	3.01	2.29	115.8	150.9
April	14.82	18.32	73.83	63.6	140.3	36.2	2.52	2.50	117.9	184.6
May	21.45	22.01	77.48	73.58	138.7	76.8	1.88	2.36	131.9	206.7
June	25.19	25.06	77.2	90.03	152.7	433.9	1.74	1.94	129.3	102.7
July	28.52	28.86	79.77	80	389.7	89.4	2.02	2.13	126.1	192.8
August	28.56	27.07	74.26	84.81	83.6	133.8	2.07	2.25	223	177
September	24.08	22.39	79.83	84.67	91	59.4	2.00	2.25	105.7	121.8
October	16.69	17.23	77.29	84.58	83.5	51.5	1.64	1.78	150.7	136.5
November	11.87	13.42	73.87	86.4	14.6	33.8	1.31	1.94	157.1	133.9
December	6.35	4.39	68.48	77.32	15.2	5.5	2.35	1.76	151.4	112.2

emissions, mesoscale circulation and changes in temperature that cause evaporation or condensation of moisture in the atmosphere. The minimum values of β refer to an ideally dust free atmosphere, while values superior to unity refer to an extremely turbid atmosphere (Mavromatakis and Franghiadakis, 2007).

A number of atmospheric turbidity indices using different methods have been introduced during the past decades in order to estimate this turbidity coefficient (Ellouz et al., 2013), for example, Dogniaux (1974) calculated the β values using an empirical formula. Among several β turbidity coefficients the most frequently used are the Louche's model (Louche et al., 1987), which has been compared in different sites around the world (Lin et al., 2016; Bilbao et al., 2014; Trabelsi and Masmoudi, 2011; Zakey et al., 2004). In this study, Louche's model is used for estimating β in Wuhan, Central China, which is based on the Iqbal C model (Iqbal, 1983) for calculating the solar irradiance. Under cloudless conditions, DNI at one site can be expressed in terms of various atmospheric transmittances, which can be written as

$$\mathrm{DNI}=0.975\ 1E_0I_0\tau_{oz}\tau_w\tau_g\tau_r\tau_a \tag{2}$$

where E_0 is the eccentricity correction factor of the Earth's orbit and I_0 is solar constant (1 367 $\mathrm{W\cdot m^{-2}}$). τ_{oz}, τ_w, τ_g, τ_r and τ_a are transmittances of ozone, water vapor, gas mixture, Rayleigh effect and aerosols, respectively.

$$\tau_{oz}=1-[0.161\ 1U_3(1+139.48U_3)^{-0.303\,5}-0.002\ 715U_3(1+0.044U_3+0.000\ 3U_3^2)^{-1}] \tag{3}$$

where $U_3=lm_r$ is the ozone relative optical path length and l is the total ozone column in cm. m_r is the relative optical mass given by Kasten (1996)

$$m_r=[\cos\theta_z+0.15(93.885-\theta_z)^{-1.253}]^{-1} \tag{4}$$

The transmittance for water vapor is expressed as Louche et al. (1987)

$$\tau_w=1-2.495\ 9wm_r[(1+79.034wm_r)^{0.682}+6.385wm_r]^{-1} \tag{5}$$

where w is the water thickness (cm). The transmittance for uniformly mixed gases is given by Bird and Hulstrom (1981)

$$\tau_g=\exp[-0.012\ 7m_a^{0.26}] \tag{6}$$

where m_a means the air mass given by $m_a=m_r(p/101\ 325)$ (p is the local pressure in Pascal). The transmittance for Rayleigh scattering is

$$\tau_r=\exp[-0.090\ 3m_a^{0.83}(1.01+m_a-m_a^{1.01})] \tag{7}$$

The transmittance for aerosols is given by

$$\tau_a=(0.124\ 4\alpha-0.016\ 2)+(1.003-0.125\alpha)\exp[-\beta m_a(1.089\alpha+0.512\ 3)] \tag{8}$$

Combing Eq. (2) to (8), β values can be finally obtained as

$$\beta=1/Am_a\ln\ [B/(C-D)] \tag{9}$$

where A, B, C and D are expressed as

$$A=1.089\alpha+0.512\ 3 \tag{10}$$

$$B=1.003-0.125\alpha \tag{11}$$

$$C=\mathrm{DNI}/0.975\ 1E_0I_S\tau_{oz}\tau_w\tau_g\tau_r \tag{12}$$

$$D=0.124\ 4\alpha-0.016\ 2 \tag{13}$$

1.3 Linke Turbidity Factor T_L

Linke's turbidity factor (T_L) is useful for modeling the atmospheric absorption and scattering of the solar radiation during cloudless skies. The value of T_L (generally vary between 1 and 10) can be derived from the direct component of the solar irradiance (Djafer and Irbah, 2013; Trabelsi and Masmoudi, 2011; Zakey et al., 2004). In the present work, turbidity coefficient T_L is calculated from

$$T_L=T_{lk}\delta_{Rk}(m_a)/\delta_{Ra}(m_a) \tag{14}$$

where T_{lk} is the Linke factor according to Kasten (1980), $\delta_{Rk}(m_a)$ is the Rayleigh integral optical thickness and $\delta_{Ra}(m_a)$ the integral optical thickness given by Louche et al. (1987) and adjusted by Kasten (1996). The Linke factor T_{lk} is related to the normal incidence solar irradiance by the equation (Djafer and Irbah, 2013; Trabelsi and Masmoudi, 2011)

$$T_{lk}=(0.9+9.4\sin h)(2\ln (I_0R_0/R)-\ln (\mathrm{DNI})) \quad (15)$$

where h is the Sun's elevation angle in degrees, R and R_0 are the instantaneous and mean Sun-Earth distances, respectively. $\delta_{Rk}(m_a)$ and $\delta_{Ra}(m_a)$ are given by the following expressions

$$\delta_{Rk}(m_a)=(9.4+0.9m_a)^{-1} \quad (16)$$

$$\delta_{Ra}(m_a)=(6.629\ 6+1.751\ 3m_a-0.120\ 2m_a^2+0.006\ 5m_a^3-0.000\ 13m_a^4)^{-1} \quad (17)$$

2 RESULTS AND DISCUSSION

Ten-minute values of the Ångström turbidity coefficient β and Linke's turbidity factor T_L under cloudless sky conditions were calculated using Eqs. (2)–(17) during 2010–2011 at Wuhan, Central China. Figure 2 shows a typical daily pattern of DNI and Ångström turbidity coefficient β for a cloudless day (2 August 2010), it is clear that β values drop a little when DNI increased sharply in the early morning; Ångström turbidity β shows fluctuations along the day, increasing in morning, remaining with fluctuations during the central part of the day and then generally decreasing in the evening. These fluctuations may be influenced by local air pollution sources, meteorological conditions and industrial activities (Wang et al., 2015c; Bilbao et al., 2014). Similar phenomenon have also been observed in Central Spain (Bilbao et al., 2014), which may due to the local high aerosol loadings and humidity in both study areas (maybe the data quality also influences the diurnal variations of β values). It is known that water vapor and cloud cover through absorption processes markedly affects the longer wavelengths, decreasing broadband solar radiation to a much greater extent, so Ångström turbidity β are generally higher in the noon time during the day.

2.1 Hourly, Daily and Monthly Values of β and T_L

The diurnal variations of both turbidity coefficients in spring, summer, autumn and winter (represented by the seasonal average values) are presented in Figs. 3 and 4, respectively. It is observed that annual mean β values generally increase from 0.28 in the morning to 0.35 at noon, then decreasing to the lowest value (0.1) in the evening during the day. There is a decrease for β values from eight o'clock to ten o'clock in Spring months, while β values increased from eight o'clock to ten o'clock in Autumn. It can also be seen that β remains nearly constant around noon at some months (for example, the summer months) and it diminishes in the evening near sunset, which is consistent with previous studies Louche et al. (1987), Pedrós et al. (1999) and Bilbao et al. (2014). The standard deviations (of β) are larger in spring and summer, which may mainly be due to the fact that more dust events and haze conditions take place in these months. Meanwhile, Fig. 4 shows that the seasonal and annual variations of T_L are similar to those shown in Fig. 3 for β, and annual mean T_L generally varies from 3 to 7 in Central China. T_L values in winter are the lowest during the year, they decrease from 5.31 at thirteen o'clock to 3.22 at 17 o'clock with average values being 4.76. The diurnal variability can be explained by the geographical location, climatic effects and characteristics of the site, for example, the increase in the turbidity in the morning may due to the increasing anthropogenic aerosols (industrial activities).

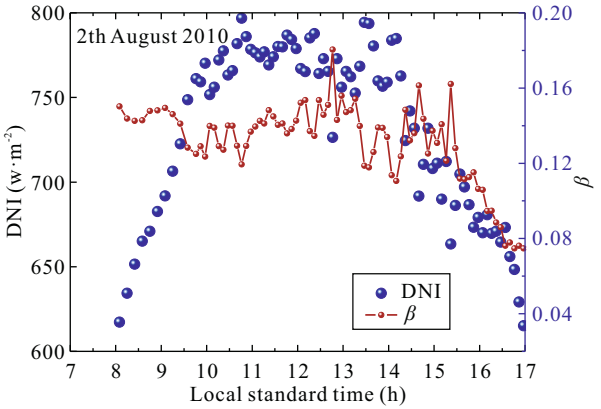

Figure 2. Diurnal variations of DNI and β for a cloudless day in Wuhan, China.

Statistical analysis has been conducted to show the frequency distribution of Ångström turbidity coefficient β and Linke's turbidity factor T_L in Central China during 2010–2011. As shown in Fig. 5, the computed β values show preponderance about 52.8% located between 0.15 and 0.35; 11% of the β values are less than 0.15, 23.9% of the β values are between 0.35 and 0.5 and only 12.3% are greater than 0.5. As regards for T_L, only 1.4% of the values are less than 3.3, 78.1% are between 3.3 and 7.7 and 20.6% exceed 7.7. These findings can be compared with results reported by other researchers in different sites around the world, Trabelsi and Masmoudi (2011) indicated that only 5% of the values of T_L are greater than 5 on the island of of Kerkennah and about 27% on Sidi Bou Saïd; about 68% of the β values range between 0.02 and 0.1 and only 7% are greater than 0.15 at Sidi Bou Saïd in Tunisia during 2008–2009. Djafer and Irbah (2013) reported that 39.8% of T_L values are less than 3, 47.5% are between 3 and 5 and only 12.7% are greater than 5; 84.8% of β values are less than 0.15 and only 15.2% are more than 0.15 over Ghardaïa City in Algeria. Large differences are also found between our observations and those in the region of Castilla and León (Spain), where 84.5% of β values are between 0.02 and 0.15 and 14.9% exceed 0.15. Heavy anthropogenic aerosols mainly derive from building construction and manufacturing industry in recent years, and the serious air pollution situations may lead to high values of T_L and β in Central China. As stated in section 2.1, the $PM_{2.5}$ mass concentration in this region was far higher than the national standards, it is reasonable to have larger values of both turbidity coefficients in Central China due to abundant of particulate pollutants in the atmosphere.

The monthly variations of Ångström turbidity coefficient β and Linke's turbidity factor T_L at Wuhan, China during 2010–2011 are shown in Fig. 6. It can be observed that there is a same trend for both turbidity coefficients along the year and they have the maximum values in spring and summer months and minimum values in winter months. Monthly mean β values increased from 0.18 in January to 0.47 in June with annual average of 0.34 in the year 2010; monthly mean daily β values in 2011 are slightly larger than those in 2010: maximum value (0.48) in May and minimum value (0.26) in December. Similarly, monthly mean T_L increased from winter to summer months with annual mean daily value being 6.7. The aerosol optical depth (AOD), including Ångström turbidity coefficient, has been investigated in different regions of China. AODs generally increase from north to south, with low values (<0.2) over the Tibetan Plateau and northwestern

China and high AODs (>0.6) in central and eastern China where industrial emissions and anthropogenic activities were likely sources (Che et al., 2015). For example, the AOD values at Beijing are 0.79, 0.75, 0.85, 0.74, 0.86 and 1.06, respectively, during 2002–2007 (Yu et al., 2009; Xia et al., 2006); the annual mean AOD was 0.6±0.3 at Nanjing during 2011–2012 (Zhuang et al., 2014). These turbidity coefficient values were also generally higher than those reported in Hong Kong, China, where monthly T_L values increased from 3.89 in January to 5.26 in May with annual mean being 4.39; monthly β values ranged from 0.115 in January to 0.18 in April with annual average of 0.132 during 1991–1999 (Li and Lam, 2002). Our results can be compared with findings around the world, for example, Thailand (Janjai et al., 2003), Egypt (El-Metwally, 2013; Zakey et al., 2004), Greece (Jacovides et al., 2005), US (López and Batlles, 2004), Spain (Bilbao et al., 2014; Djafer and Irbah, 2013) and Tunisia (Trabelsi and Masmoudi, 2011). These comparisons can be used for evaluating atmospheric conditions in different regions, which will be of vital importance for early warning and control of air pollutions.

2.2 Relationship between Turbidity Coefficients and Meteorological Parameters

It is known that meteorological conditions, such as temperature and relative humidity are major parameters determining the variations of β and T_L. Figure 7 shows the relationships between hourly values of β and T_L and humidity and temperature, respectively, in Wuhan, Central China. Both turbidity coefficients almost increase linearly with humidity, reaching the highest values when humidity is about 62.5%, and then decrease slightly with humidity. At the same time, both turbidity coefficients generally increase with temperature, but there are some fluctuations in the variation patterns, for example, β values suddenly decrease in some extent at 16 °C, as shown in Fig. 7. These change patterns may be due to the combined effects of local meteorological parameters, for example, the air does contain more water vapor due to higher temperature, so turbidity coefficients will be higher at some extent (Trabelsi and Masmoudi, 2011).

The wind direction and wind speed are also important factors in governing the spatio-temporal variation of turbidity. In this paper, hourly mean wind direction was used to analyze the

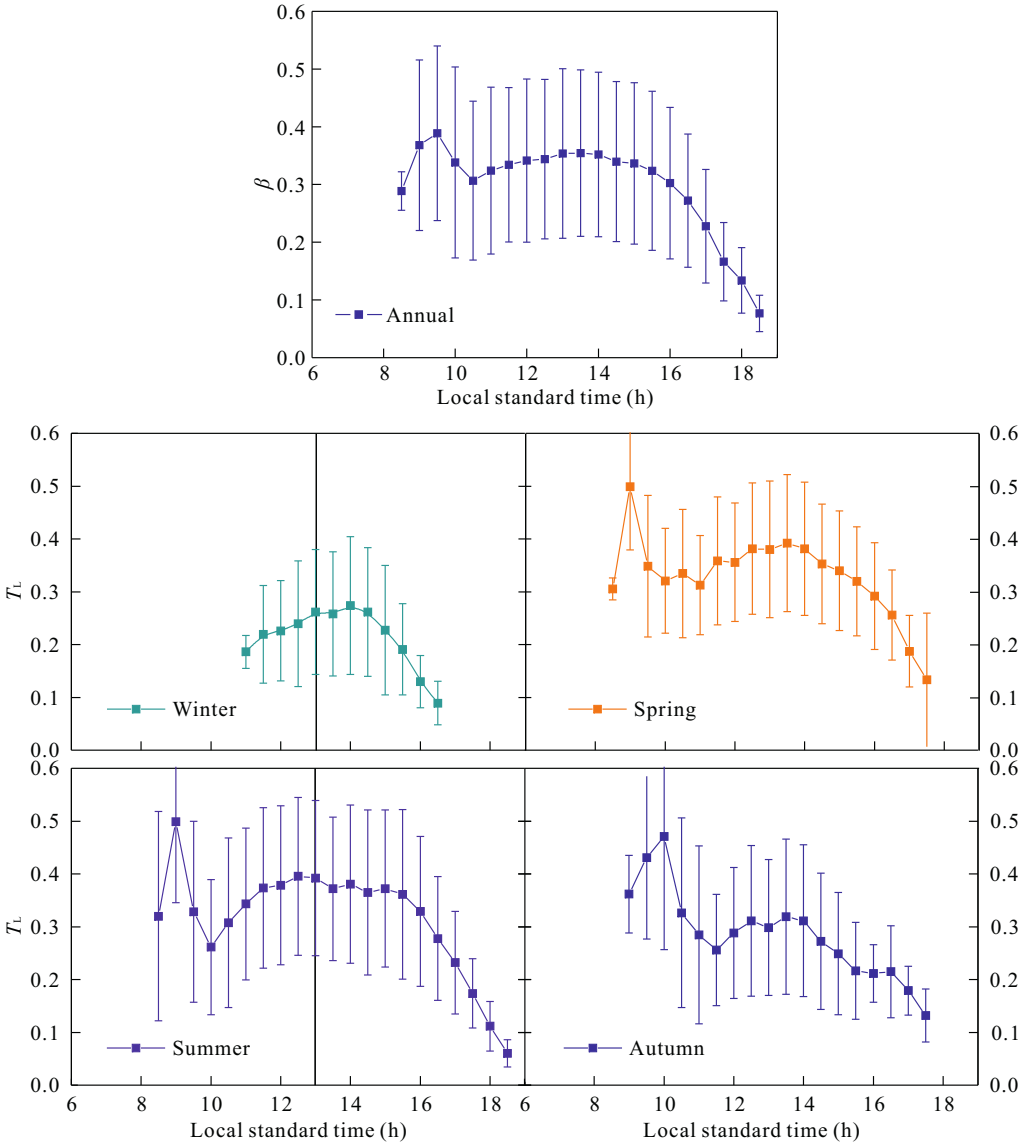

Figure 3. The diurnal variations of annual and seasonal Ångström turbidity coefficient β in Wuhan, China.

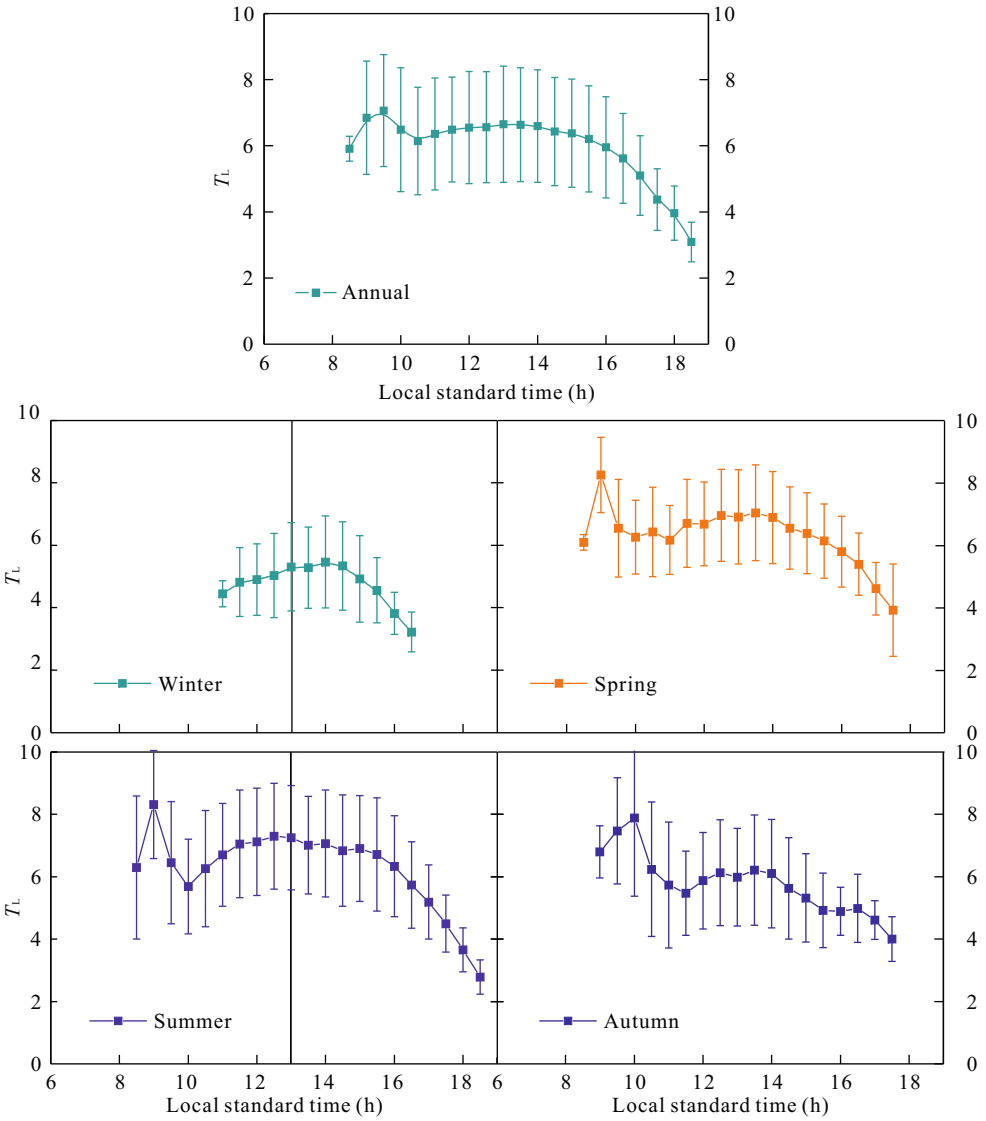

Figure 4. The diurnal variations of annual and seasonal Linke's turbidity factor T_L in Wuhan, China.

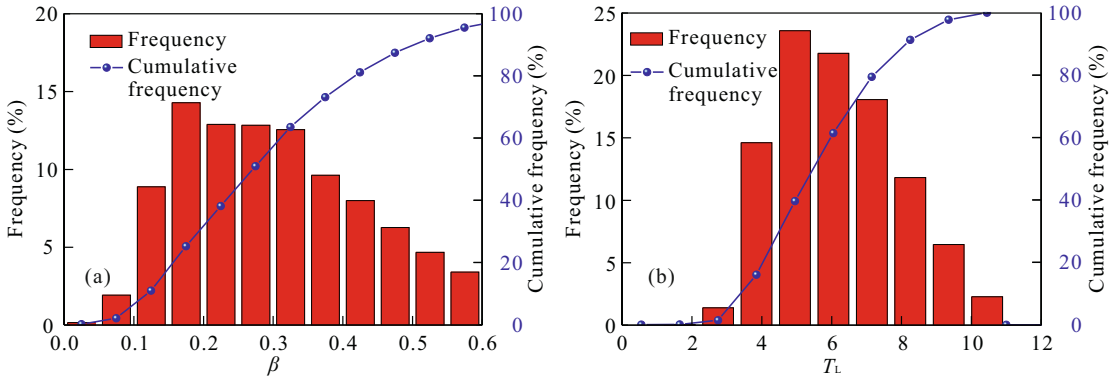

Figure 5. Frequency distribution of Ångström turbidity coefficient β and Linke's turbidity factor T_L in Central China.

frequency of different wind directions and their effects on both turbidity coefficients. Figure 8a shows the frequency distribution of various wind directions and the associated β values in Central China during 2010–2011 (NE, E, SE, S, SW, W, NW and N mean wind direction with northeast, east, southeast, south, southwest, west, northwest and north, respectively). It can be observed that N and S are the prevailing wind directions (42%), followed by NE, SW and E. The β values under various wind directions are all located between 0.3 and 0.36 and β values under N, NE and NW are slightly larger than other wind directions. This is partly due to the dust events in northern China in spring and early summer. Moreover, we analyze the frequency distributions of wind directions in each range of β values (Fig. 8b), it can be seen that SW and S are the main wind directions

when β values are lower than 0.25, this conditions mostly appear in the later summer and autumn months due to the Southwest Monsoon from the Indian Ocean. N, NE and S are the prevailing winds when β values are greater than 0.25, which may partly due to dust events in northern China in spring months and the Southeast Monsoon from western Pacific Ocean in summer. It should be noted that the above seasonal β values are related to the concentration of aerosols in the air, which mainly depends on the pollution situation of the local or regional area of Wuhan, China. For example, the previous studies have indicated the monthly variations of concentration of aerosols are mainly due to the pollutant particles emitted from local sources, dust particles by the long-range transport and weather conditions, and the anthropogenic fine-mode particles are the dominated aerosol components. So studies are still needed to clarify the aerosol sources and related chemical compositions in further.

3 CONCLUSIONS

Ground-based measurements of solar radiation and meteorological parameters from 2010 to 2011 at Wuhan University are used to study the hourly, daily and monthly variations of Ångström turbidity coefficient β and Linke turbidity factor T_L. It

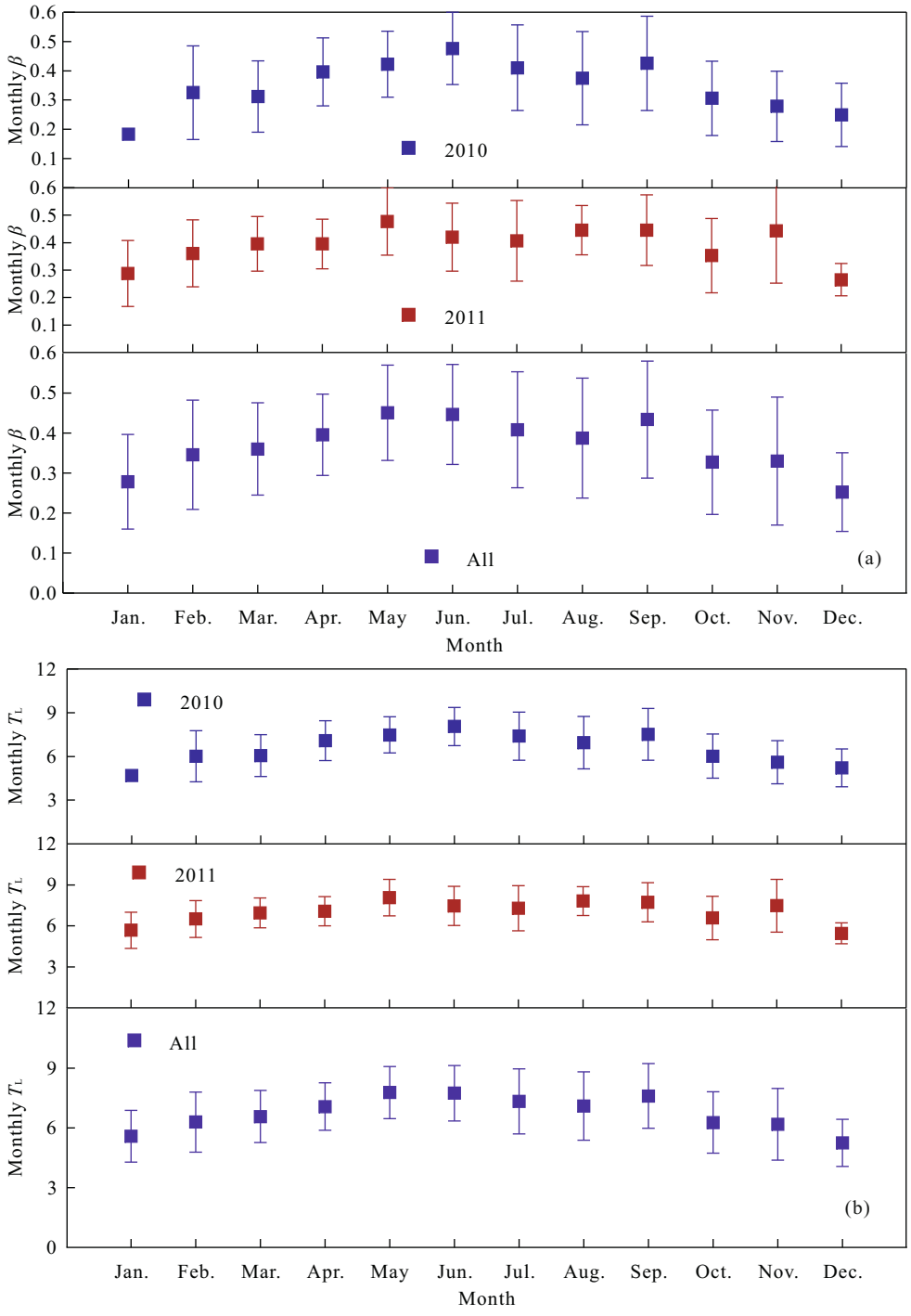

Figure 6. Monthly variations of mean Ångström turbidity coefficient β in Central China.

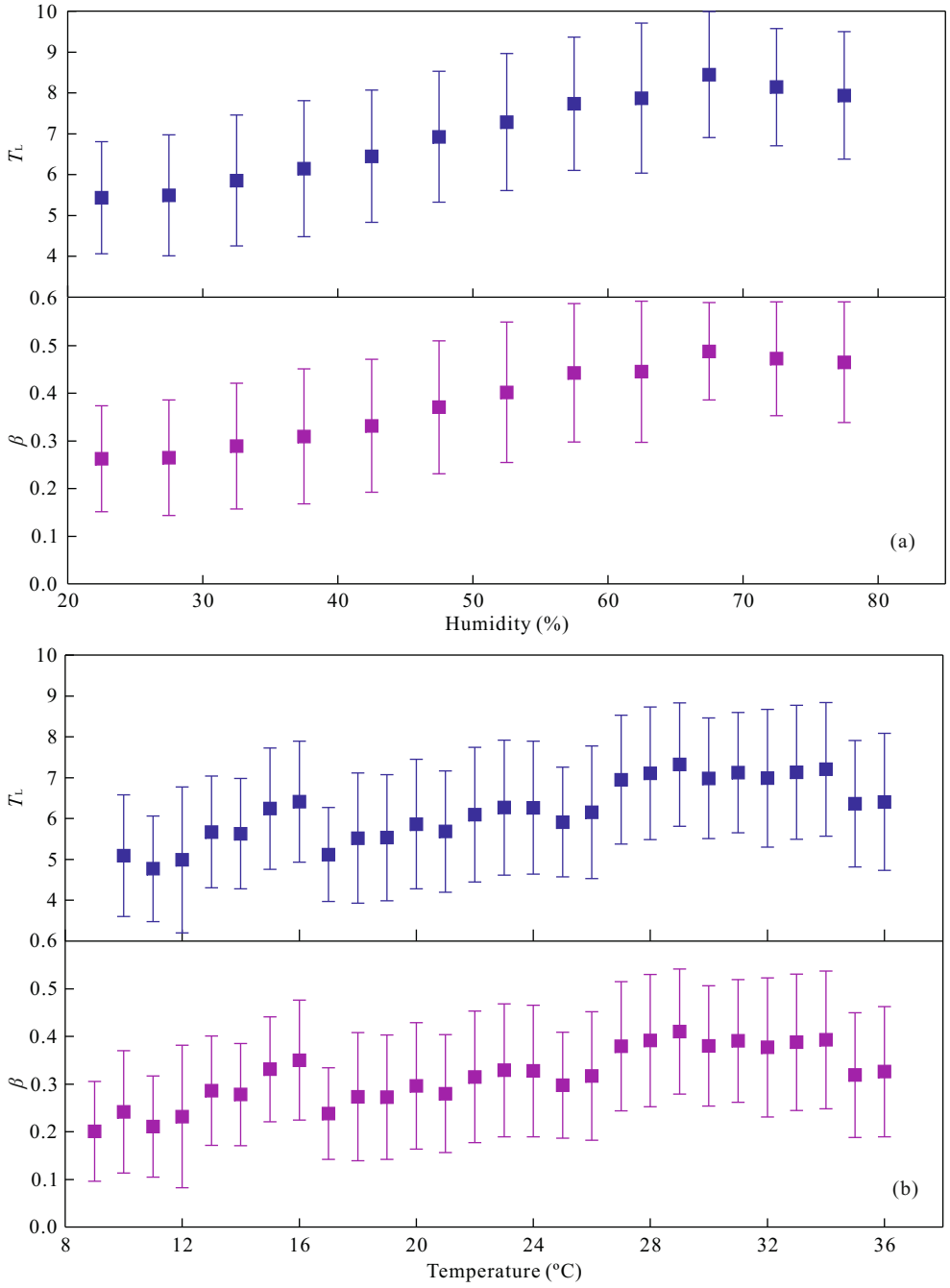

Figure 7. Relationship between turbidity coefficients and main meteorological parameters.

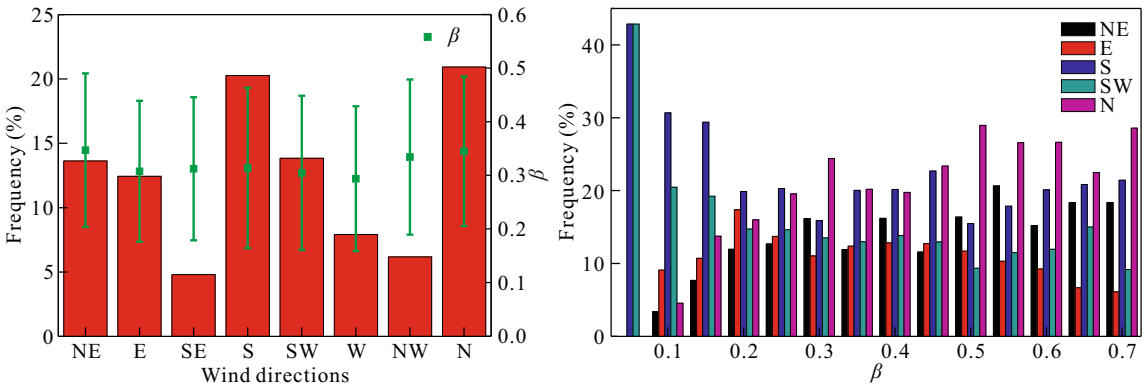

Figure 8. Frequency distribution of various wind directions and the associated β values in Central China.

was found that both turbidity coefficients have the same diurnal and seasonal variation patterns, for example, annual mean β and T_L generally reach the higher values at noon during the day. Monthly mean daily β values increased from 0.25 in December to 0.45 in May with annual average of 0.36 for the whole study period. Maximum values of T_L are also observed in spring and summer months, while minimum values appear in winter months. These seasonal variations is highly associated with local geographical conditions, climatic characteristics and air pollution sources, for example, large turbidity coefficients in spring and summer months may be due to more dust events and haze conditions during this period.

Statistical analysis indicates that β values show preponderance (52.8%) between 0.15 and 0.35, 78.1% of T_L values are between 3.3 and 7.7. Our results have been compared with different sites around the world, including Beijing, Nanjing, Tibetan Plateau, northwestern China and central and eastern China, Hong Kong, Thailand, Egypt, Athens, Spain, and Africa, which indicate the turbidity coefficients are higher in Central China due to the serious air pollution situations. The relationships between turbidity coefficients and humidity and temperature have also been analyzed, and it is observed that both turbidity coefficients generally increase linearly with humidity and temperature in Central China. Finally, N and S are found as the prevailing wind directions (42%) in the study area, the dependence of β values on various wind directions has been investigated. It reveals that SW and W are the main wind directions when β values are less than 0.25 in the later summer and autumn months due to the Southwest Monsoon from the Indian Ocean; N and NE are the prevailing winds when β values are greater than 0.25 in spring due to the effects of dust events in northern China.

Atmospheric turbidity coefficients are important parameters influencing the solar radiation reaching the Earth's surface under cloudless sky conditions. This study analyzes the turbidity coefficients from measured direct normal irradiance in Central China for the first time, which may contribute to regional atmospheric environment, solar energy application and climate change studies. Much work still needs to be done in future, for example, the estimating algorithms will be improved and compared with other methods for comprehensive understanding.

ACKNOWLEDGMENTS

This work was financially supported by the National Natural Science Foundation of China (No. 41601044), the Special Fund for Basic Scientific Research of Central Colleges, China University of Geosciences, Wuhan (Nos. CUG150631, 009-162301124611), and the 111 Project (No. B08030). The final publication is available at Springer via http://dx.doi.org/10.1007/s12583-017-0756-2.

REFERENCES CITED

Adamopoulos, A. D., Kambezidis, H. D., Kaskaoutis, D. G., et al., 2007. A Study of Aerosol Particle Sizes in the Atmosphere of Athens, Greece, Retrieved from Solar Spectral Measurements. *Atmospheric Research*, 86(3/4): 194–206. doi:10.1016/j.atmosres.2007.04.003

Ångström, A., 1961. Techniques of Determinig the Turbidity of the Atmosphere. *Tellus*, 13(2): 214–223. doi:10.3402/tellusa.v13i2.9493

Ångström, A., 1964. The Parameters of Atmospheric Turbidity. *Tellus*, 16(1): 64–75. doi:10.1111/j.2153-3490.1964.tb00144.x

Bilbao, J., Román, R., Miguel, A., 2014. Turbidity Coefficients from Normal Direct Solar Irradiance in Central Spain. *Atmospheric Research*, 143: 73–84. doi:10.1016/j.atmosres.2014.02.007

Bird, R. E., Hulstrom, R. L., 1981. A Simplified Clear Sky Model for Direct and Diffuse Insolation on Horizontal Surfaces. SERI/TR-642-761 Solar Energy Research Institute, Colorado

Braslau, N., Dave, J. V., 1973. Effect of Aerosols on the Transfer of Solar Energy through Realistic Model Atmospheres. Part I: Non-Absorbing Aerosols. *Journal of Applied Meteorology*, 12(4): 601–615. doi:10.1175/1520-0450(1973)012<0601:eoaott>2.0.co;2

Chaâbane, M., 2008. Analysis of the Atmospheric Turbidity Levels at Two Tunisian Sites. *Atmospheric Research*, 87(2): 136–146. doi:10.1016/j.atmosres.2007.08.003

Che, H., Zhang, X. Y., Xia, X., et al., 2015. Ground-Based Aerosol Climatology of China: Aerosol Optical Depths from the China Aerosol Remote Sensing Network (CARSNET) 2002–2013. *Atmospheric Chemistry and Physics*, 15(13): 7619–7652. doi:10.5194/acp-15-7619-2015

Djafer, D., Irbah, A., 2013. Estimation of Atmospheric Turbidity over Ghardaïa City. *Atmospheric Research*, 128: 76–84. doi:10.1016/j.atmosres.2013.03.009

Dogniaux, R., 1974. Representation Analytique des Composantes du Rayonnement Solaire. Institut Royal de Météorologie de Belgique, Série A, No. 83

Ellouz, F., Masmoudi, M., Medhioub, K., 2013. Study of the Atmospheric Turbidity over Northern Tunisia. *Renewable Energy*, 51: 513–517. doi:10.1016/j.renene.2008.04.035

El-Metwally, M., 2013. Indirect Determination of Broadband Turbidity Coefficients over Egypt. *Meteorology and Atmospheric Physics*, 119(1/2): 71–90. doi:10.1007/s00703-012-0223-7

Feng, Q., Wu, S. J., Du, Y., et al., 2010. Variations of PM_{10} Concentrations in Wuhan, China. *Environmental Monitoring and Assessment*, 176(1/2/3/4): 259–271. doi:10.1007/s10661-010-1581-6

Gong, W., Zhang, M., Han, G., et al., 2015. An Investigation of Aerosol Scattering and Absorption Properties in Wuhan, Central China. *Atmosphere*, 6(4): 503–520. doi:10.3390/atmos6040503

Grenier, J. C., De La Casinière, A., Cabot, T., 1995. Atmospheric Turbidity Analyzed by Means of Standardized Linke's Turbidity Factor. *Journal of Applied Meteorology*, 34(6): 1449–1458. doi:10.1175/1520-0450(1995)034<1449:atabmo>2.0.co;2

Gueymard, C. A., 2005. Importance of Atmospheric Turbidity and Associated Uncertainties in Solar Radiation and Luminous Efficacy Modelling. *Energy*, 30(9): 1603–1621. doi:10.1016/j.energy.2004.04.040

Gueymard, C. A., Garrison, J. D., 1998. Critical Evaluation of Precipitable Water and Atmospheric Turbidity in Canada Using Measured Hourly Solar Irradiance. *Solar Energy*, 62(4): 291–307. doi:10.1016/s0038-092x(98)00005-x

Hu, B., Wang, Y. S., Liu, G. R., 2007. Spatiotemporal Characteristics of Photosynthetically Active Radiation in China. *Journal of Geophysical Research*, 112(D14): D14106. doi:10.1029/2006jd007965

Hussain, M., Khatun, S., Rasul, M. G., 2000. Determination of Atmospheric Turbidity in Bangladesh. *Renewable Energy*, 20(3): 325–332. doi:10.1016/s0960-1481(99)00102-0

Iqbal, M., 1983. An Introduction to Solar Radiation. Academic Press, New York

Jacovides, C. P., Kaltsounides, N. A., Asimakopoulos, D. N., et al., 2005. Spectral Aerosol Optical Depth and Angstrom Parameters in the Polluted Athens Atmosphere. *Theoretical and Applied Climatology*, 81(3/4): 161–167. doi:10.1007/s00704-004-0110-3

Janjai, S., Kumharn, W., Laksanaboonsong, J., 2003. Determination of Angstrom's Turbidity Coefficient over Thailand. *Renewable Energy*, 28(11): 1685–1700. doi:10.1016/s0960-1481(03)00010-7

Kaskaoutis, D. G., Kambezidis, H. D., 2007. Comparison of the Ångström Parameters Retrieval in Different Spectral Ranges with the Use of Different Techniques. *Meteorology and Atmospheric Physics*, 99(3/4): 233–246. doi:10.1007/s00703-007-0279-y

Kasten, F., 1980. A Simple Parameterization of the Pyrheliometric Formula for Determining the Linke Turbidity Factor. *Meteor. Rundschau*, 33: 124–127

Kasten, F., 1996. The Linke Turbidity Factor Based on Improved Values of the Integral Rayleigh Optical Thickness. *Solar Energy*, 56(3): 239–244. doi:10.1016/0038-092x(95)00114-7

Leckner, B., 1978. The Spectral Distribution of Solar Radiation at the Earth's Surface—Elements of a Model. *Solar Energy*, 20(2): 143–150. doi:10.1016/0038-092x(78)90187-1

Li, D. H. W., Lam, J. C., 2002. A Study of Atmospheric Turbidity for Hong Kong. *Renewable Energy*, 25(1): 1–13. doi:10.1016/s0960-1481(01)00008-8

Li, K. M., Li, Z. Q., Wang, C. Y., et al., 2016. Shrinkage of Mt. Bogda Glaciers of Eastern Tian Shan in Central Asia during 1962–2006. *Journal of Earth Science*, 27(1): 139–150. doi:10.1007/s12583-016-0614-7

Lin, A. W., Zou, L., Wang, L., et al., 2016. Estimation of Atmospheric Turbidity Coefficient over Zhengzhou during 1961–2013. *Renewable Energy*, 86: 1134–1144

Linke, F., 1922. Transmissions Koeffizient und Trubungsfaktor. *Beitraége Zur Physik der Atmosphaére*, 10: 91–103

Long, C. N., Ackerman, T. P., 2000. Identification of Clear Skies from Broadband Pyranometer Measurements and Calculation of Downwelling Shortwave Cloud Effects. *Journal of Geophysical Research*: *Atmospheres*, 105(D12): 15609–15626. doi:10.1029/2000jd900077

López, G., Batlles, F. J., 2004. Estimate of the Atmospheric Turbidity from Three Broad-Band Solar Radiation Algorithms: A Comparative Study. *Annales Geophysicae*, 22(8): 2657–2668. doi:10.5194/angeo-22-2657-2004

Louche, A., Maurel, M., Simonnot, G., et al., 1987. Determination of Ångström's Turbidity Coefficient from Direct Total Solar Irradiance Measurements. *Solar Energy*, 38(2): 89–96. doi:10.1016/0038-092x(87)90031-4

Malik, A. Q., 2000. A Modified Method of Estimating Ångström's Turbidity Coefficient for Solar Radiation Models. *Renewable Energy*, 21(3/4): 537–552. doi:10.1016/s0960-1481(00)00080-x

Mavromatakis, F., Franghiadakis, Y., 2007. Direct and Indirect Determination of the Linke Turbidity Coefficient. *Solar Energy*, 81(7): 896–903. doi:10.1016/j.solener.2006.11.010

Pan, Z. T., Zhang, Y. J., Liu, X. D., et al., 2016. Current and Future Precipitation Extremes over Mississippi and Yangtze River Basins as Simulated in CMIP5 Models. *Journal of Earth Science*, 27(1): 22–36. doi:10.1007/s12583-016-0627-2

Pedrós, R., Utrillas, M. P., Martínez-Lozano, J. A., et al., 1999. Values of Broad Band Turbidity Coefficients in a Mediterranean Coastal Site. *Solar Energy*, 66(1): 11–20. doi:10.1016/s0038-092x(99)00015-8

Power, H. C., 2001. Estimating Atmospheric Turbidity from Climate Data. *Atmospheric Environment*, 35(1): 125–134

Salazar, G. A., 2011. Estimation of Monthly Values of Atmospheric Turbidity Using Measured Values of Global Irradiation and Estimated Values from CSR and Yang Hybrid Models. Study Case: Argentina. *Atmospheric Environment*, 45(15): 2465–2472. doi:10.1016/j.atmosenv.2011.02.048

Salazar, G., Utrillas, P., Esteve, A., et al., 2013. Estimation of Daily Average Values of the Ångström Turbidity Coefficient β Using a Corrected Yang Hybrid Model. *Renewable Energy*, 51: 182–188

Sapkota, B., Dhaubhadel, R., 2002. Atmospheric Turbidity over Kathmandu Valley. *Atmospheric Environment*, 36(8): 1249–1257. doi:10.1016/s1352-2310(01)00582-9

Trabelsi, A., Masmoudi, M., 2011. An Investigation of Atmospheric Turbidity over Kerkennah Island in Tunisia. *Atmospheric Research*, 101(1/2): 22–30. doi:10.1016/j.atmosres.2011.03.009

Trenberth, K. E., Fasullo, J. T., Kiehl, J., 2009. Earth's Global Energy Budget. *Bulletin of the American Meteorological Society*, 90(3): 311–323. doi:10.1175/2008bams2634.1

Wang, L. C., Gong, W., Li, C., et al., 2013. Measurement and Estimation of Photosynthetically Active Radiation from 1961 to 2011 in Central China. *Applied Energy*, 111: 1010–1017. doi:10.1016/j.apenergy.2013.07.001

Wang, L. C., Gong, W., Ma, Y. Y., et al., 2014a. Photosynthetically Active Radiation and Its Relationship with Global Solar Radiation in Central China. *International Journal of Biometeorology*, 58(6): 1265–1277. doi:10.1007/s00484-013-0690-7

Wang, L. C., Gong, W., Li, J., et al., 2014b. Empirical Studies of Cloud Effects on Ultraviolet Radiation in Central China. *International Journal of Climatology*, 34(7): 2218–2228. doi:10.1002/joc.3832

Wang, L. C., Gong, W., Xia, X. G., et al., 2015a. Long-Term Observations of Aerosol Optical Properties at Wuhan, an Urban Site in Central China. *Atmospheric Environment*, 101: 94–102. doi:10.13039/501100001809

Wang, L. C., Gong, W., Ramesh, P., et al., 2015b. Aerosol Optical Properties over Mount Song, a Rural Site in Central China. *Aerosol and Air Quality Research*, 15: 2051–2064. doi:10.4209/aaqr.2014.12.0335

Wang, L. C., Salazar, G. A., Gong, W., et al., 2015c. An Improved Method for Estimating the Ångström Turbidity Coefficient β in Central China during 1961–2010. *Energy*, 81: 67–73. doi:10.13039/501100001809

Wang, L. C., Kisi, O., Zounemat-Kermani, M., et al., 2016. Solar Radiation Prediction Using Different Techniques: Model Evaluation and Comparison. *Renewable and Sustainable Energy Reviews*, 61: 384–397. doi:10.1016/j.rser.2016.04.024

Wang, Y. Q., Zhang, X. Y., Sun, J. Y., et al., 2015. Spatial and Temporal Variations of the Concentrations of PM_{10}, $PM_{2.5}$ and PM_1 in China. *Atmospheric Chemistry and Physics Discussions*, 15(11): 15319–15354. doi:10.13039/501100004751

Wen, C. C., Yeh, H. H., 2009. Analysis of Atmospheric Turbidity Levels at Taichung Harbor near the Taiwan Strait. *Atmospheric Research*, 94(2): 168–177. doi:10.1016/j.atmosres.2009.05.010

Wild, M., Gilgen, H., Roesch, A., et al., 2005. From Dimming to Brightening: Decadal Changes in Solar Radiation at Earth's Surface. *Science*, 308(5723): 847–850. doi:10.1126/science.1103215

Xia, X. A., Chen, H. B., Wang, P. C., et al., 2006. Variation of Column-Integrated Aerosol Properties in a Chinese Urban Region. *Journal of Geophysical Research*, 111(D5): D05204. doi:10.1029/2005jd006203

Xia, X. G., Li, Z. Q., Holben, B., et al., 2007. Aerosol Optical Properties and Radiative Effects in the Yangtze Delta Region of China. *Journal of Geophysical Research*, 112(D22): D22S12. doi:10.1029/2007jd008859

Yu, X. N., Zhu, B., Zhang, M. G., 2009. Seasonal Variability of Aerosol Optical Properties over Beijing. *Atmospheric Environment*, 43(26): 4095–4101. doi:10.1016/j.atmosenv.2009.03.061

Zakey, A., Abdelwahab, M., Makar, P. A., 2004. Atmospheric Turbidity over Egypt. *Atmospheric Environment*, 38(11): 1579–1591

Zhuang, B. L., Wang, T. J., Li, S., et al., 2014. Optical Properties and Radiative Forcing of Urban Aerosols in Nanjing, China. *Atmospheric Environment*, 83: 43–52. doi:10.13039/501100001809